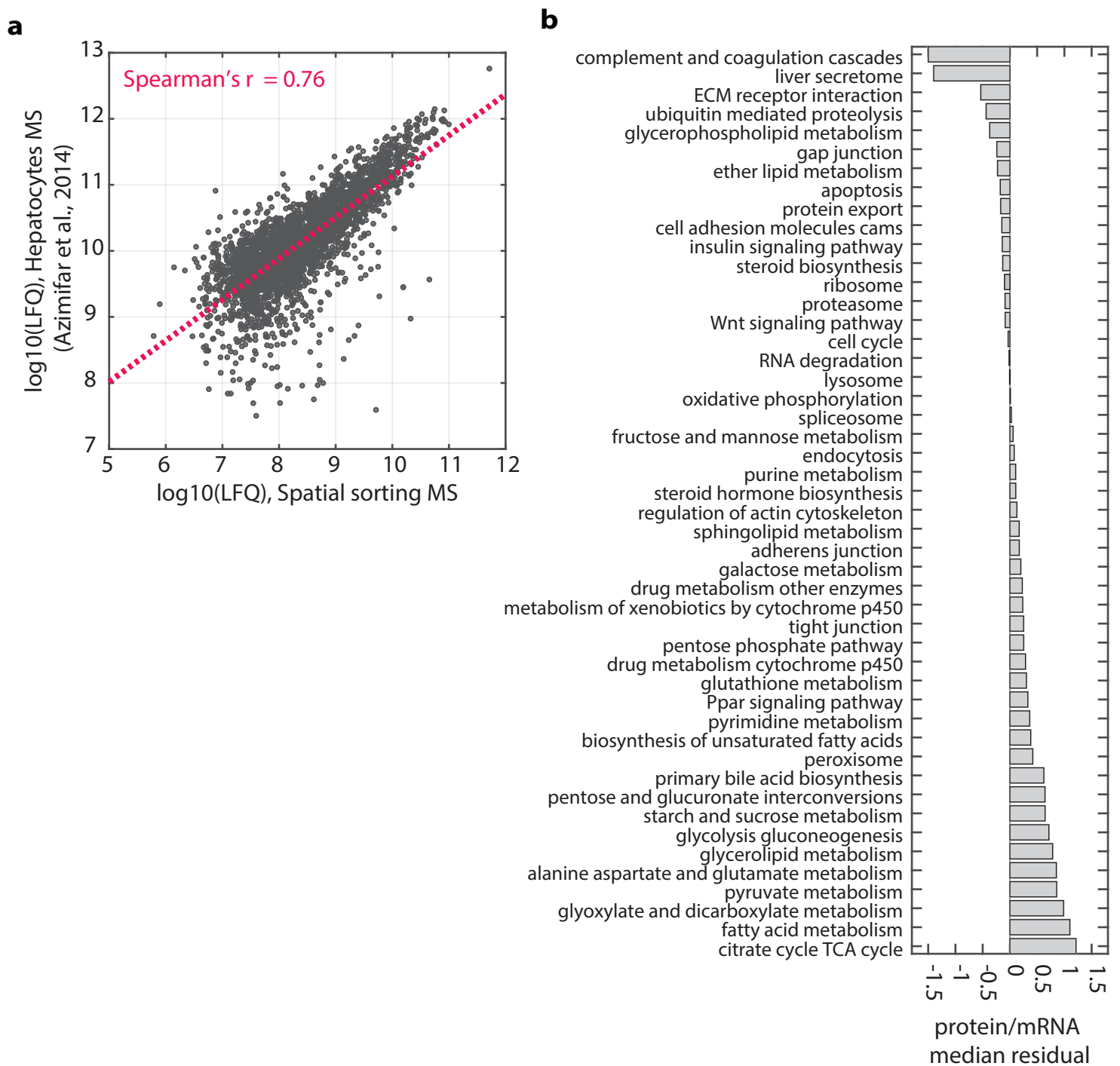
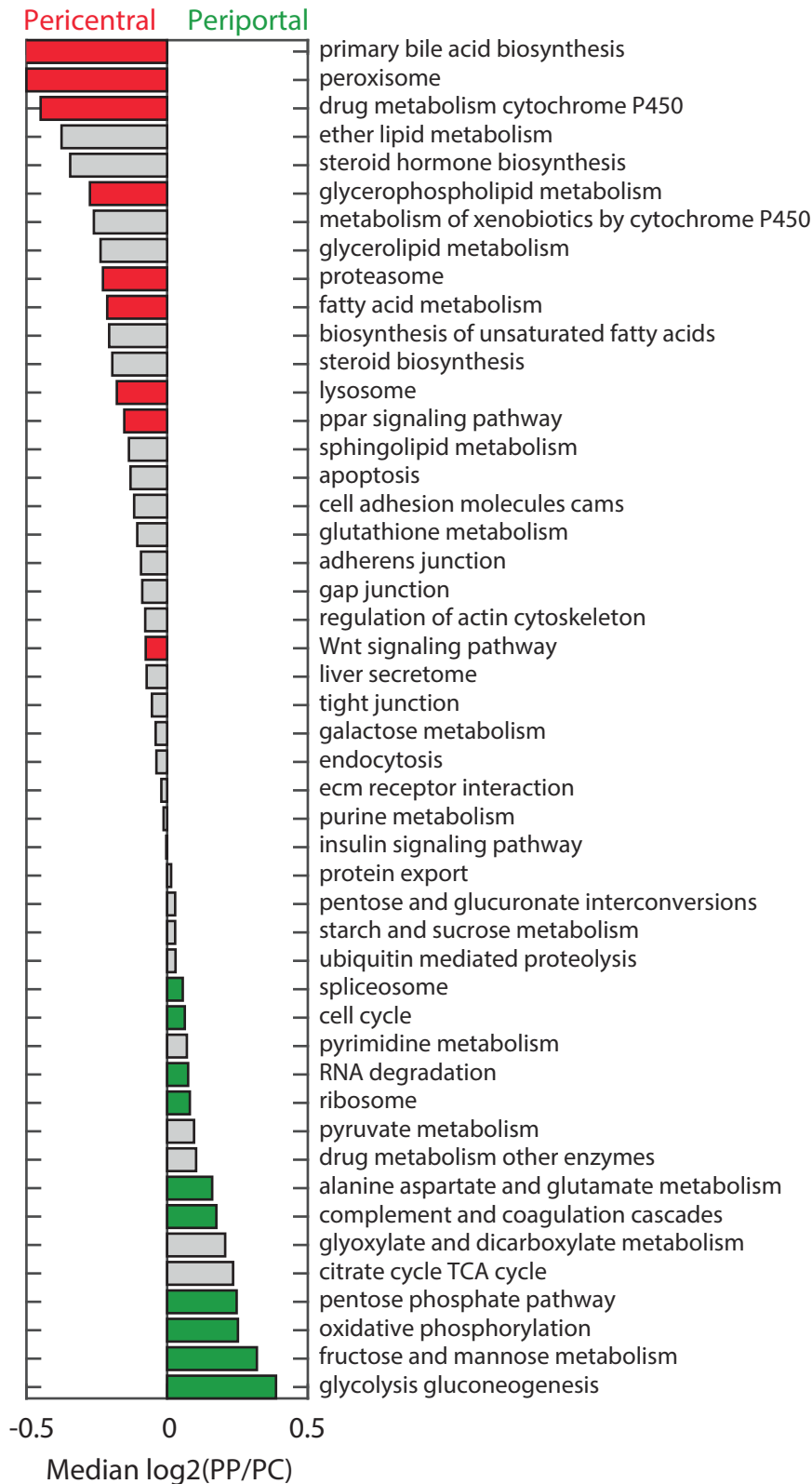


Supplementary Fig. 1 | Surface markers candidates for spatial sorting and ploidy gating in FACS.

a, Surface markers zonation profiles. Data from 5. Expression is normalized to the maximal level for each gene. Genes are sorted by expression center of mass. **b**, Gating for single cells. After the first gating of hepatocytes (fig. 3a), we applied two additional gates to eliminate doublet cells. First gate was according to the area and width of the forward scatter (left panel) and second gate was according to the area and width of the side scatter (right panel). FACS gates were similar in all five experiments. **c-d**, Gating by ploidy levels. FACS gates were similar in all five experiments. **c**, Histogram of cells according to Hoechst stains, proportional to DNA content, each peak represents a different ploidy class with different proportions in the hepatocytes population. Red – diploid cells, orange – tetraploid cells, blue – octoploid cells. **d**, distribution of hepatocytes according to E-cadherin and CD73 intensities, stratified by ploidy class. Red and green rectangles are 1 and 8 gates selected for the 4n hepatocytes.

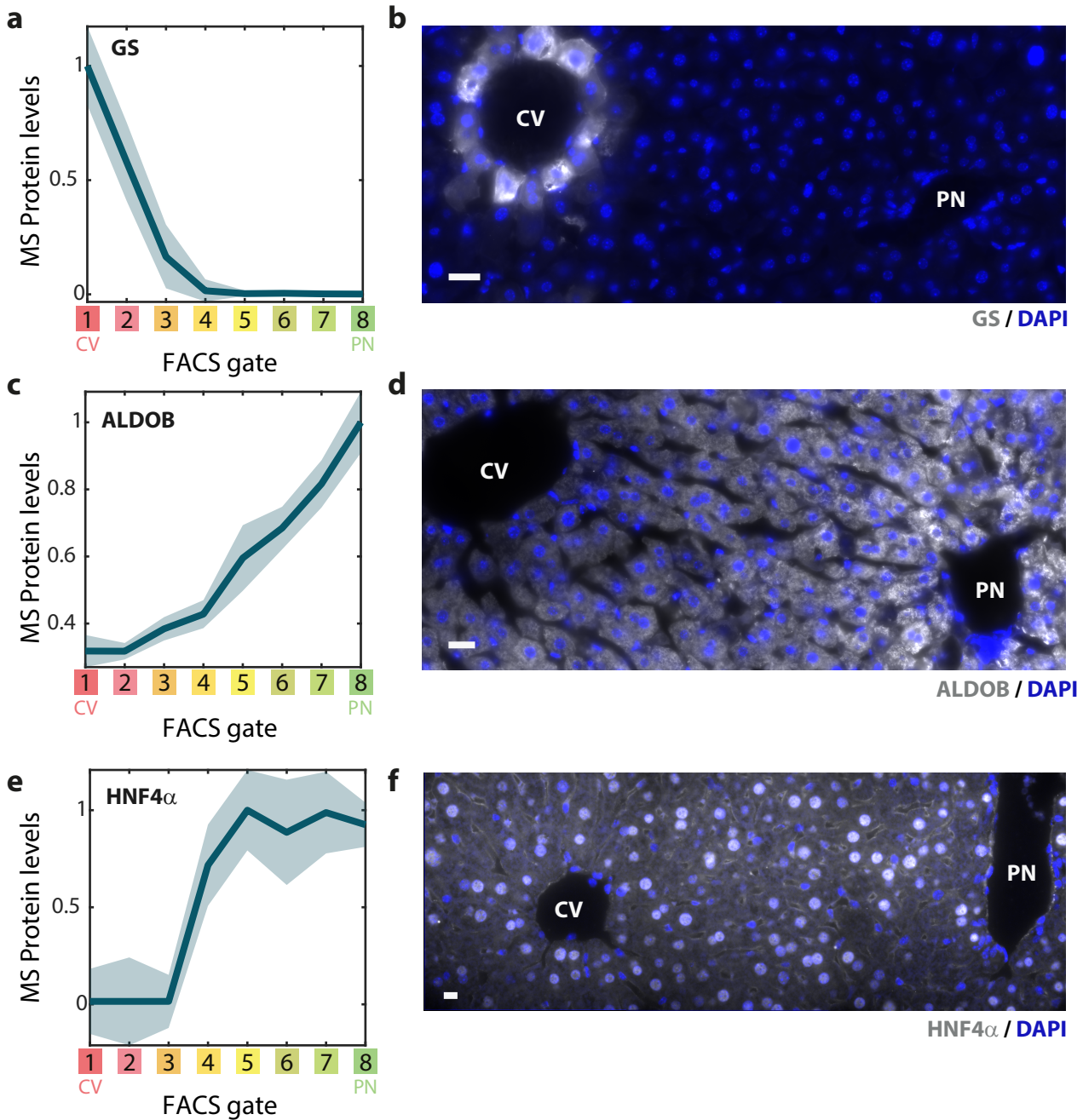


Supplementary Fig. 2 | Comparisons of proteomic dataset. **a**, Scatter plot of log₁₀(LFQ) of mean proteins over all FACS gates for 5 mice and log₁₀(LFQ) of previously published mouse hepatocytes mass-spec. measurements¹². Red dashed line marks the regression line, Spearman's $r=0.76$. Number of proteins = 2831. **b**, Protein to mRNA residuals from regression line, bar represent median of genes belonging to the KEGG pathway. See main Fig. 4.



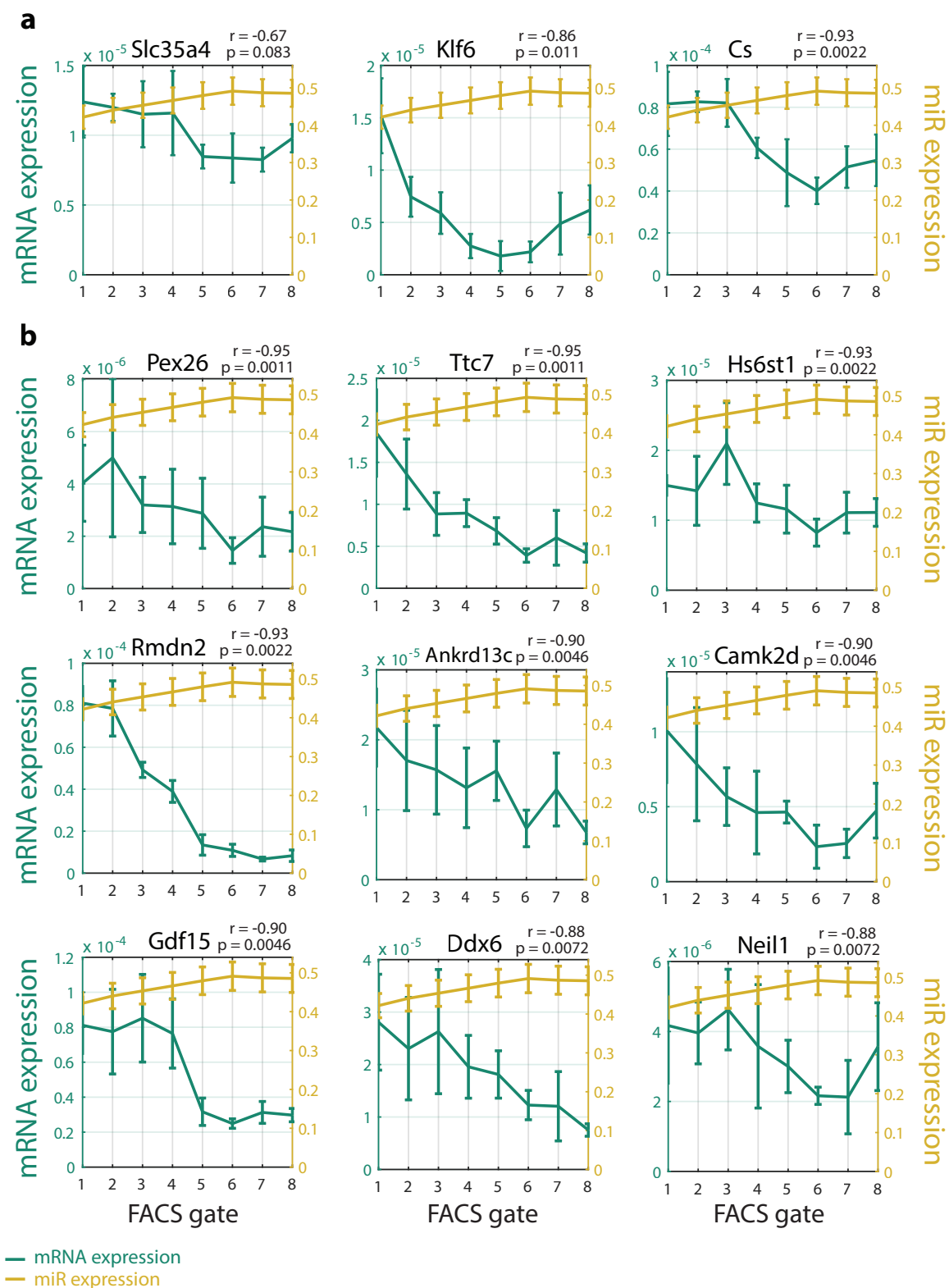
Supplementary Fig. 3 | Zonation of hepatocyte proteome by KEGG pathways.

Median log₂ of ratio between periportal and pericentral gates of proteins belonging to the selected KEGG families over the 5 mice. Colored bars represent KEGG pathways with FDR < 0.2 of p-values obtained from two-sided single sample sign rank test for each of the KEGG pathways. Red represent negative log₂ ratio, indicating pericentral enrichment, and green represent positive values, indicating periportal enrichment.



Supplementary Fig. 4 | Immuno-Fluorescence of selected proteins validates proteins zonation.

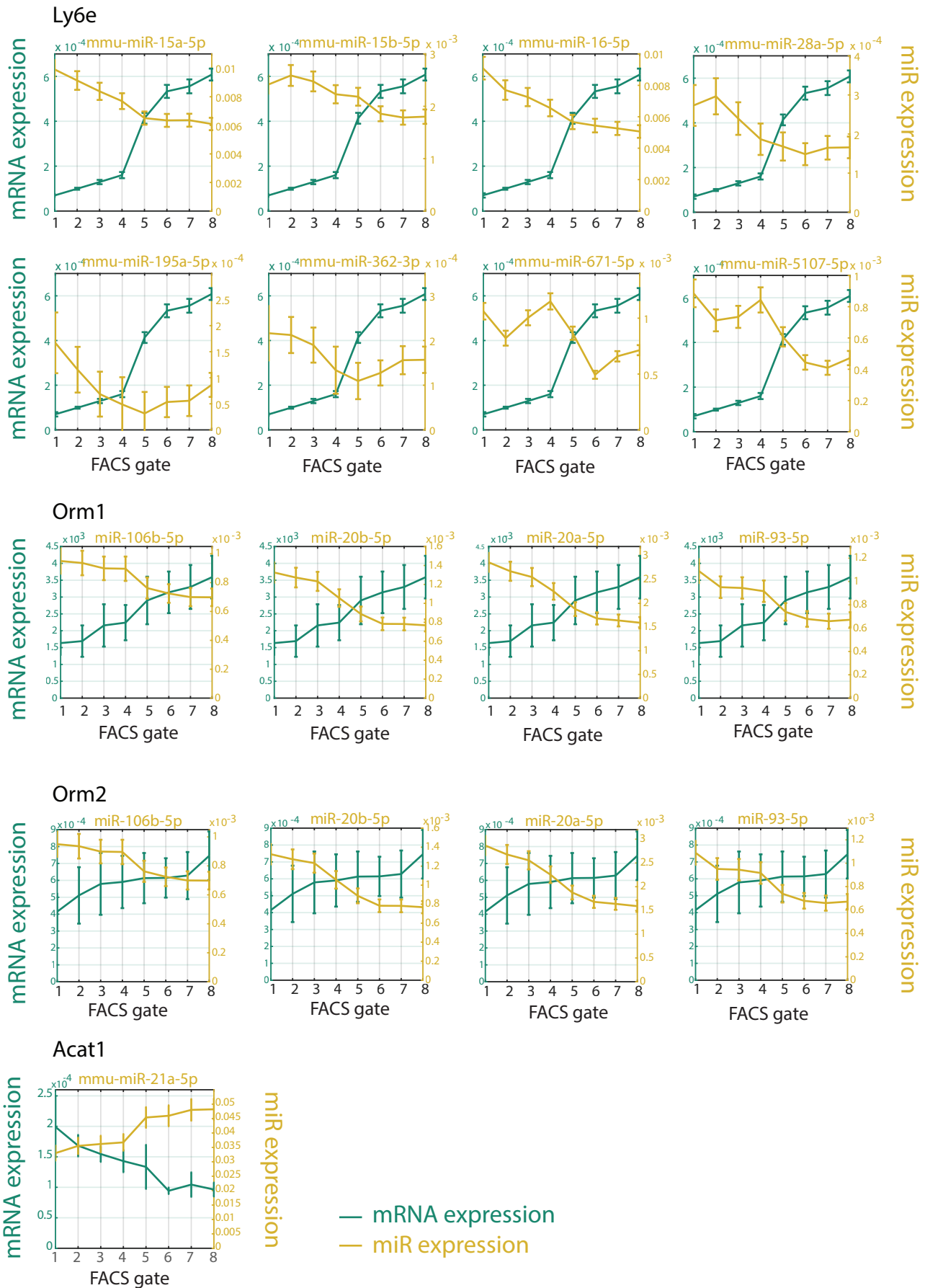
Protein levels of three proteins - Glutamine synthetase (GS) (a-b), Aldolase b (ALDOB) (c-d) and HNF4 α (e-f). Graphs (a,c,e) presenting protein levels according to mass-spectrometry (MS) results in the eight zoned FACS gates populations. Protein levels are normalized to the maximal expression level of each protein across the eight populations. N=5 mice. Lines indicate means and patches indicate SEM. Images (b,d,f) are representative IF lobule scans showing gradients of proteins (white) along the protocentral axis. Blue – DAPI. CV – central vein, PN – portal node, scale bar – 10 μ m. IF experiments were performed on two mice in total for GS and ALDOB with similar results and three mice for HNF4 α with similar results.



Supplementary Fig. 5 | Selected anti-correlated target genes of miR-122-5p.

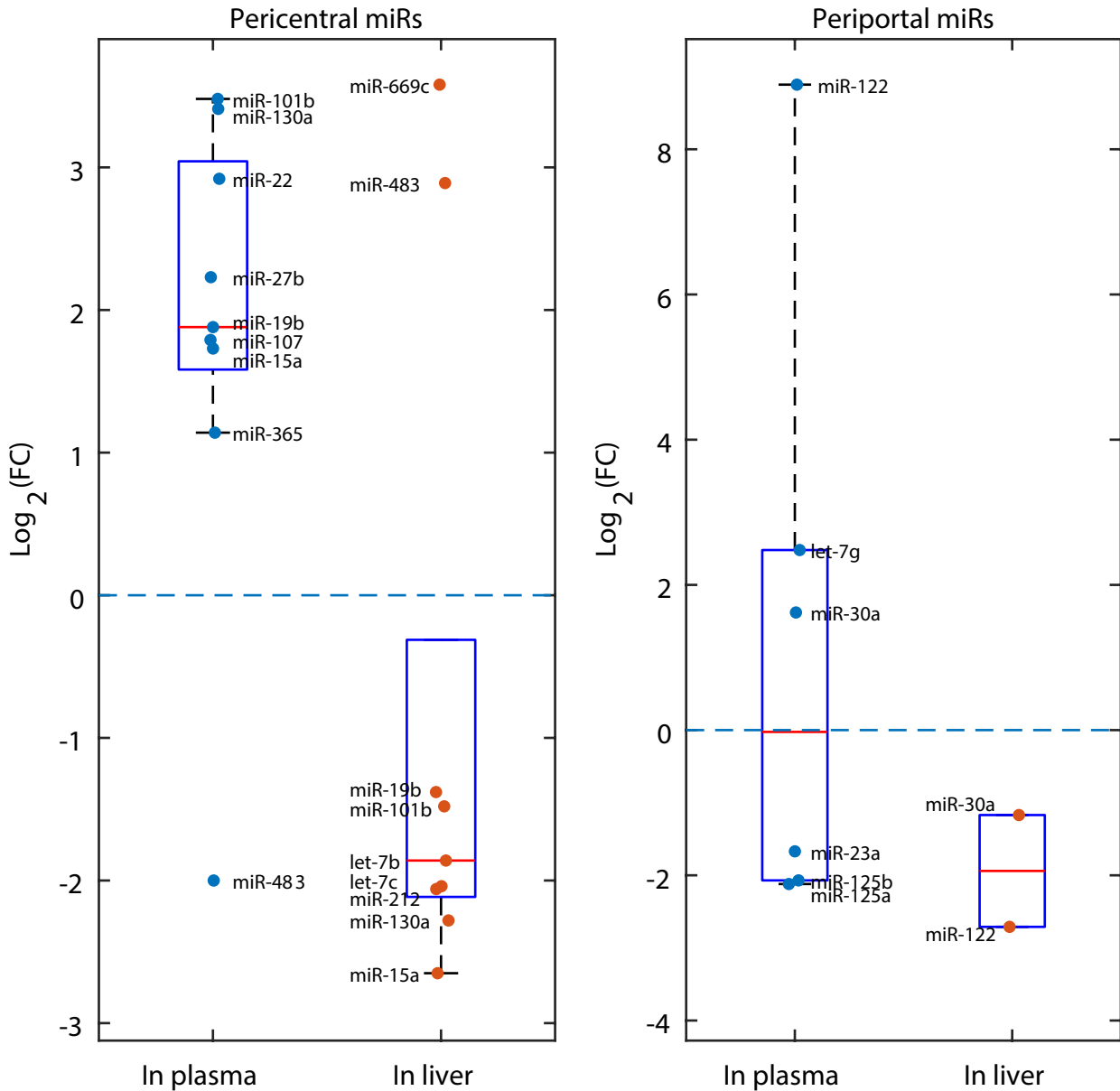
a, miR-122-5p was found to be anti-correlated with some of its canonical targets, *Slc35a4*, *Klf6* and *Cs* (following 29,77). **b**, Top nine anti-correlated predicted targets of miR-122-5p.

Expression is normalized to the sum. Lines represent mean of 5 mice for mRNA (green) and 3 mice for miRNA (yellow). Error bars are SEM. Shown are Spearman correlations and their respective p-values, computed using exact permutation distributions.



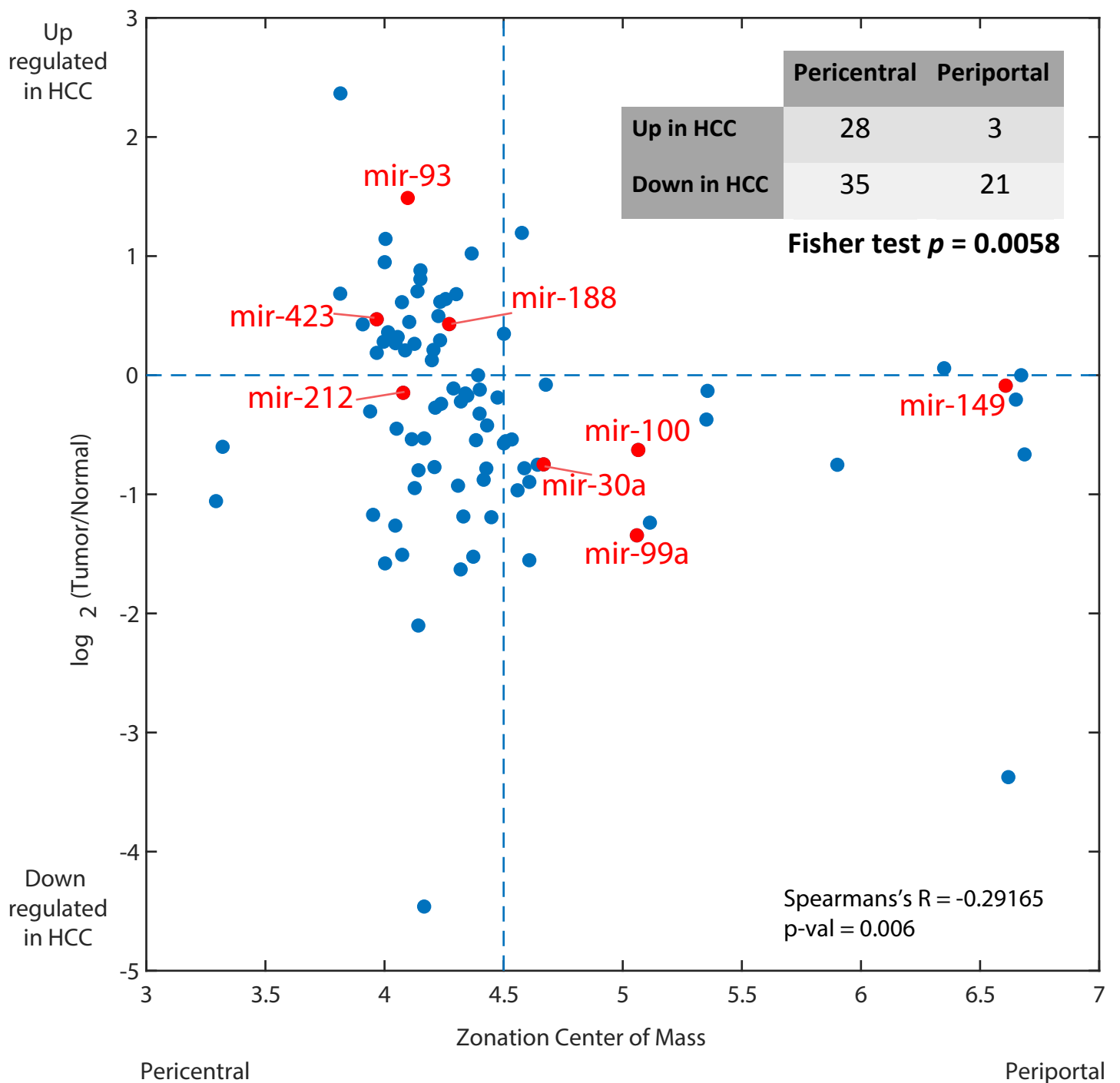
Supplementary Fig. 6 | Target genes significantly anti-correlated with their potential regulating miRNAs. Expression is normalized to the sum. Lines represent mean of 5 mice for mRNA (green) and 3 mice for miRNA (yellow). Error bars are SEM.

Fold change in miRNA abundance following APAP treatment



Supplementary Fig. 7 | Pericentrally-zonated miRNA are enriched in the plasma of mice undergoing pericentral damage via acetaminophen (APAP) overdose.

Shown are fold-changes of miRNA levels in blood plasma and liver of APAP-treated in mice, relative to controls, stratified by zonation. Pericentral miRNA have zonation center of mass smaller than 4.5 and zonation FDR ≤ 0.2 , periportal miRNA have zonation center of mass larger than 4.5 and zonation FDR ≤ 0.2 . miRNA levels in APAP-treated mice were obtained from Wang et al. (2009)⁴⁶, n=4 mice. a, Pericentral miRNAs are more abundant in plasma and less abundant in liver of APAP-treated mice (two-tailed Wilcoxon $p = 0.050$). b, Periportal miRNAs are not significantly more abundant in plasma compared to liver tissue (two-tailed Wilcoxon $p = 0.43$). Horizontal red lines are medians, boxes denote 25-75 percentiles, whiskers are 1.5x inter quartile range.



Supplementary Fig. 8 | Periportally-zonated miRNA are down-regulated in hepatocellular carcinoma.

The log₂ fold change of miRNAs in HCC tumors (n = 372 TCGA tumor samples) compared to normal samples (n = 50 TCGA normal samples) is plotted against the miRNAs' expression center of mass. Dashed line mark no zonation in the x-axis and no change it tumors in the y-axis. Red – miRNAs with predicted Wnt component targets, found in TargetScan. P-value of Spearman correlation was computed using exact permutation distributions, with a two-tailed hypothesis.